

**NONLINEAR IMPACT ANALYSIS OF
INTERNATIONAL SPACE STATION ALPHA MODULE BERTHING
USING MSC/NASTRAN**

Timothy S. West*, David A. VanHorn**, John R. LeCour*, and Mitchell W. Usrey**

McDonnell Douglas Aerospace
Space Station Division, Houston, Texas

ABSTRACT

MSC/NASTRAN nonlinear gap element modelling techniques were implemented to analyze the impact between berthing modules and on-orbit structure during assembly of International Space Station Alpha (ISSA). Component mode synthesis techniques were used to create superelements to reduce the analysis set degrees of freedom during the nonlinear analysis. Superelements were again used in structural response recovery, where the impact forces were applied to the reduced ISSA model in modal transient analysis and responses were recovered for a large number of response items. This procedure is illustrated with three different examples.

* Senior Engineer
** Engineer Specialist

INTRODUCTION

The International Space Station Alpha (ISSA) is assembled in low earth orbit over a five year period with multiple assembly flights delivering modules provided by the United States, Europe, Japan, and Russia (Figure 1). Modules provided by the United States, Europe, and Japan are normally positioned for attachment by a robotic arm without contact between the module and the on-orbit structure. A capture latching mechanism then grapples the module and retracts to pull it into the proper attachment location. However, impact may occur between the module and structure during positioning, and these impact loads are important to the design of ISSA [1]. Since the berthing modules and on-orbit structure exhibit a wide variety of dynamic characteristics over the range of configurations, detailed analyses are necessary for many berthing events. These events must be analyzed in a computationally efficient manner for accurate design loads and fatigue spectra prediction.

MSC/NASTRAN (v. 67r2) Nonlinear Transient Analysis (Solution 129) was implemented to calculate the impact forces between the berthing module and the on-orbit structure. As is true for any nonlinear analysis, computational demands tend to grow tremendously with the size and complexity of the problem. To facilitate the immense size of the ISSA finite element models (FEMs), MSC/NASTRAN component mode synthesis (CMS) model reduction techniques were used in conjunction with the nonlinear transient analysis to calculate the berthing contact interface forces. Contact surfaces were modeled with CGAP elements (nonlinear contact elements). The responses of these elements were recovered as the impact forces and applied to a higher fidelity model in MSC/NASTRAN (v. 67r2) Modal Transient Analysis (Solution 112) to calculate structural responses. This procedure is illustrated with three diverse ISSA berthing scenarios.

SOLUTION APPROACH

The primary goal of this berthing analysis was to provide accurate results for the overall structural members rather than members close to the impact location, and high frequency impact transients were a secondary concern. CGAP elements were chosen to model the berthing contact surfaces because the stiffness curve of the CGAP element (Figure 2) could be directly employed at the interface [2]. Furthermore, the interface stiffness properties of the berthing module were included in the CGAP elements to greatly improve the convergence of the solution without sacrificing important frequency content.

Structural and control system interaction effects of the robotic arm were excluded from this early analysis, but will be evaluated with respect to current uncertainties and analysis speed in the future. Conservatism was preserved by using worst case contact velocities and rigid module representation.

Once FEMs are developed for all components, the procedure consists of four steps: berthing module reduction and interface modelling, on-orbit structure reduction, impact force recovery, and structural response recovery.

Berthing Module Model Reduction and Interface Modelling

The berthing module was reduced from a multi-degree of freedom FEM to rigid mass properties and interface flexibility. The mass and inertia terms for the module were placed at the center of mass for the module, G_{cg} . Points of contact at the interface, G_i , and a point representing the center of the berthing interface, G_c , were chosen and all points were rigidly connected.

The berthing interface was modelled using CGAP elements between the chosen contact points on the berthing module and on-orbit structure. The mating contact points were defined at coincident locations, and coordinate systems were created that defined the orientation of the contact surfaces. Initial separation of the surfaces was defined with initial gap openings, U_0 , on the PGAP entry (gap element property entry). All CGAP element orientation coordinate systems were referenced to a single interface coordinate system, making the entire interface model portable to any compatible location.

The interface flexibility was statically calculated for the berthing module primary structure near the berthing interface and included on the gap closed stiffness, K_A . Engineering judgment was used to select structure for static analysis based on the relative flexibility and configuration of structure near the interface. The selected structure was analyzed statically to determine the stiffness of the interface in the impact directions, and this stiffness was then added in series with any additional stiffness not modelled in the FEM to determine K_A . The gap open stiffness, K_B , was set to a value low enough to prevent gap open forces from affecting the overall system response within the analysis envelope, but as high as possible to aid in solution convergence. Friction was ignored for this contact analysis because very little surface-to-surface sliding contact takes place. Parameters were set on the PGAP entry to allow small penetrations for penalty value adjustment, and 10% adjustment of adaptive penalty values. In addition, the gap preload, F_0 , was set to the product of K_B and U_0 to balance the problem on the first time step [3].

This reduced berthing model was coupled with a rigid interface and sanity checked with a nonlinear transient analysis. The results of this analysis were compared with conservation of momentum calculations to ensure correct modelling of the impact.

On-Orbit Structure Model Reduction

The on-orbit structure FEM was reduced to minimize the number of analysis degrees of freedom in the nonlinear and modal transient analyses using MSC/NASTRAN CMS techniques [4 - 6]. The ISSA component FEMs were reduced to superelements with their points connecting with neighboring ISSA components defined as the boundary set. The cutoff frequency for the module containing the berthing interface was approximately 50 Hz to capture the high frequencies associated with berthing events, while other components had a cutoff frequency of approximately 30 Hz. This integrated on-orbit structural analysis model was used in the modal transient analysis for structural loads recovery, but was further reduced to an external superelement for use as the nonlinear analysis model. The boundary of this superelement consisted of the berthing contact points, where the interface model was later attached for impact analysis. By previous studies [7], residual structure cutoff frequencies for both the structural and the nonlinear analysis models were set to 15 Hz for large configurations, and 20 Hz for smaller configurations.

Interface Force Recovery

The completed models were coupled to develop the nonlinear analysis model, and interface impact forces and berthing module accelerations were calculated with free-free boundary conditions using nonlinear transient analysis [2, 3]. Initial contact velocities were assigned to the center of the berthing interface, G_C , and initial gap openings were set on the PGAP entries to simulate initial displacements and rotations. The analysis time step size was chosen to provide an adequate trace of the impact forces. Because the loading consists of short duration impacts, time step adjustment was disabled for accurate calculation of the impact forces. Adaptive time integration (bisection) and dynamic matrix updates were included for efficient convergence, and the convergence criteria was varied to achieve a solution. Damping was included as 1% of critical at the center of the frequency range of interest (g-type damping, [2]). The analysis was

conducted within the guide surface envelope, and included time necessary to capture the initial closing impact forces and any subsequent guide contacts. The resulting gap element impact forces and berthing module accelerations were used in design-to loads assessment for the berthing interface and module internal structure.

Transient Loads Recovery

The impact forces were applied to the reduced on-orbit ISSA model using modal transient analysis [2, 4, 6] to calculate internal structural responses with the modal displacement recovery method on a truncated set of modes to minimize computation time [7]. The analysis was conducted for a duration sufficient to ensure the decay of all modal responses, which was generally 20 times the duration of the nonlinear analysis. Modal damping was set to 1% of critical for all modes. Transient responses and peak loads were recovered for up to 14,500 items for use in fatigue analysis and design-to loads assessment.

EXAMPLES

Three examples of berthing scenarios on ISSA are presented to illustrate the diverse contact interfaces and structural configurations analyzed by this procedure. The S3/S4 truss segment is part of the structural backbone of ISSA and is attached with a segment-to-segment attach system (SSAS). The Japanese Experiment Module-Pressurized Module (JEM-PM) is a pressurized habitation and experiment module and is attached with a Common Berthing Mechanism (CBM). Finally, the Unpressurized Logistics Carrier (ULC) is a general unpressurized cargo carrier and is attached with a ULC attach structure (ULCAS). Several model and analysis parameters are listed in Table 1 for comparison and are discussed in the following sections.

S3/S4 Truss Segment Berthing

The S3/S4 truss segment contained the starboard solar alpha rotary joint and starboard inboard electric power system, and had a total weight of 31,000 lbs. The segment berthed to the SSAS on the starboard end of the S1 segment (Figure 3). The on-orbit structure weighed 645,000 lbs including the Orbiter (224,000 lbs), which was docked to the forward port of the forward Resource Node.

The SSAS between the S3/S4 and S1 segments was composed of three guide pins and cones that align the interfaces, and four motor bolt cups and cones at the truss bulkhead corners for seating the interfaces together (Figure 4). Three grids located at the guide cone vertices and four grids located at the segment bulkhead corners were chosen as the berthing contact points, G_i , and were rigidly connected to the interface center point, G_c . This point was rigidly attached to the center of mass, where the rigid mass properties were placed. Contact between each guide pin and cone was modelled with four intersecting CGAP elements that formed an inverted pyramid, and contact between each motor bolt cup and cone was modelled with a single CGAP element in the closing direction. The truss bay adjacent to the berthing interface was chosen to represent the S3/S4 interface flexibility. This structure was statically analyzed in the contact directions and the gap closed stiffness for each element was set to these values. The guide pins were modelled directly with bar type elements between the cone gap elements and the reduced on-orbit structure for element loads recovery during the impact analysis. The guide pins and cone vertices were initially separated slightly more than the motor bolt cups and cones, allowing complete mating of the interface without bottoming out the guide pins. Contact was simulated only while the guide pin tips were within three inches of the guide cone vertices in the closing direction due to geometry of the guide cones.

The analysis set sizes of the structural analysis and nonlinear analysis models created for the on-orbit configuration of Figure 3 are listed in Table 1. The contact points at the guide pin roots and truss corners of the structural analysis model were placed in the boundary set during the CMS reduction to form the nonlinear analysis model. This 79% reduction in model size made multiple solutions of this problem feasible.

Four different combinations of initial rates were applied to G_c to maximize guide cone and motor bolt impacts. The convergence criteria was set to load and work error tests for solution convergence. A typical S3/S4 segment impact was analyzed for five seconds in real time with a time step size of 0.01 seconds. As presented in Table 1, the relatively small analysis set size and large integration time step produced the fastest solution time among the three cases listed. A typical force time history for guide cone and motor bolt contact is shown in Figure 5. In this case, initial guide pin/cone contact induced a rotation of the segment, and severe impact occurred at the motor bolt. This impact resulted in a large shear load on the base of the photo voltaic array mast at the opposite end of the truss, located over 170 feet away. The impact forces were then applied to the structural analysis model in modal transient analysis for 82 seconds of real time and 6,400 load items were recovered.

Japanese Experiment Module - Pressurized Module Berthing

The JEM-PM was the heaviest pressurized module at 39,000 lbs. It was berthed to the starboard Common Berthing Mechanism (CBM) of the forward Resource Node (Figure 6). The on-orbit structure weighed 700,000 lbs including the Orbiter (224,000 lbs), which was docked to the forward port of the forward Resource Node.

The CBM was composed of two large mating rings with petal type guides to align the interfaces (Figure 7). Eight contact points, G_i , were chosen near the edges of the guides where guide contact would occur. These eight grids were rigidly attached to the interface center, G_c , which was rigidly attached to the center of mass where the mass properties were placed. Direct ring-to-ring contact was modelled with eight CGAP elements aligned in the closing direction. The end cone of the module and the CBM passive half were chosen to represent the interface flexibility for these elements because of their softness relative to the main body of the module. Therefore, their gap closed stiffness was set to the statically calculated stiffness of these components. Initial gap openings were set at zero to insure initial ring-to-ring contact for conservatism. Guide-to-guide contact was modelled with eight additional CGAP elements aligned tangential to the ring circumference. The gap closed stiffness of these elements was set as the shear stiffness of the guides because of their softness relative to the surrounding structure. By design, the CBM guides could contact simultaneously at only two of the eight guide contact locations, thus the initial gap opening was set to double the nominal mating tolerance on alternating element pairs. The guides also projected one inch perpendicular to the ring surface on each half of the CBM before sloping apart, therefore contact was analyzed only within this two inch ring-to-ring separation envelope.

The analysis set sizes of the structural analysis and nonlinear analysis models created for the on-orbit configuration of Figure 6 are listed in Table 1. The berthing port grid of the structural analysis model was placed in the boundary set during the CMS reduction to form the nonlinear analysis model. An 81% reduction in model size was achieved for this model to speed the nonlinear analysis.

The nonlinear analysis was generally performed for four seconds of real time, with a step size of 0.0025 seconds. This problem consumed the greatest computation time of the three listed in Table 1 because of a large analysis set size and a very small relative time step. Eight sets of initial conditions were used to vary the lateral rotation of the berthing module and maximize

ring-to-ring impact forces at different locations about the ring. The convergence criteria was set to load and work error tests for solution convergence. Typical time histories for ring-to-ring and guide-to-guide impact forces are shown in Figure 8. In general, the impact magnitude and duration was driven by the interface stiffness, but the effects of on-orbit structure configuration and on-orbit structural flexibility could be seen in two ways. First, overall force magnitudes were affected by the configuration of the on-orbit modules; in particular, the presence of a module on the port opposite the active berthing port. In this case, no module was present on the port side CBM of the forward Resource Node, so force magnitudes were lower. However, the presence of the Orbiter on an adjacent port near the berthing port helped increase the impact magnitudes. Second, the secondary impact pulse in the axial time history of Figures 8a and 8b was a unique result of the on-orbit structure responding to the initial impact and rebounding to strike the berthing module again. Figures 8c and 8d illustrate multiple guide-to-guide impacts as the bodies separate. This set of impact forces was then applied to the structural analysis model in a modal transient analysis for a real-time duration of 82 seconds, and 10,500 response items were recovered.

Unpressurized Logistics Carrier Berthing

The Unpressurized Logistic Carrier (ULC) may carry several attached payloads for a total weight of 19,000 lbs. The ULC berthed to the ULC Attach Structure (ULCAS) located on the port-side truss just inboard the solar alpha rotary joint (SARJ) (Figure 9). The analysis was performed on the completely assembled ISSA which had a total mass of 1,025,000 lbs including the Orbiter (224,000 lbs), and was the largest on-orbit configuration analyzed.

The berthing interface was composed of three sets of V-guides, trunnion pins, and scuff plates that form a triangle as shown in Figure 10. One contact point, G_i , was chosen on each trunnion pin to represent both trunnion pin and scuff plate contact with the V-guide, and these were rigidly connected to the interface center point, G_c . This point was rigidly attached to the center of mass point where the rigid mass properties were placed. Contact with the two arms of each V-guide was modelled by two intersecting CGAP elements forming the "V", and contact with the scuff plate was modelled by one CGAP element oriented perpendicular to the V-guide. The ULC was a very stiff structure, and the trunnion pins and scuff plates were much stiffer than the surrounding structure. Therefore, the gap closed stiffness was set approximately two orders of magnitude greater than the statically calculated flexibility of the ULCAS to provide a conservative estimate of the ULC interface flexibility. The V-guide gap elements were given initial openings vertically from the V-guide vertices, and the scuff plates were given initial openings laterally from the V-guide vertices according to mechanism mating tolerance. Geometry of the V-guides dictated that impact could only be analyzed while the trunnion pins were located vertically within two inches of the V-guide vertices.

The analysis set sizes of the structural analysis and nonlinear analysis models created for the on-orbit configuration of Figure 9 are listed in Table 1. The three grids at the vertices of the V-guides on the structural analysis model were placed in the boundary set during the CMS reduction to form the nonlinear analysis model. Multiple solutions of this large model were made possible by this 82% reduction in model size.

Several different combinations of initial rates were applied to G_c to maximize impact with the V-guides collectively and individually. The convergence criteria was set to displacement error test to obtain solution convergence. A typical ULC impact was analyzed for five seconds in real time with a time step size of 0.01 seconds. Note that this problem required much more computation time than the S3/S4 segment berthing because of a relatively large analysis set size. A typical force time history for V-guide and scuff plate contact is shown in Figure 11. The trunnion pin impacts surface A of the V-guide initially yielding the largest impact, and then small contacts

occur between scuff plate/V-guide and trunnion pin/V-guide surface B as the trunnion pin exits the V-guide. The impact forces were applied to the structural analysis model in a modal transient analysis for 82 seconds of real time and approximately 14,500 load items were recovered.

RESULTS DISCUSSION

The model and analysis parameters presented in Table 1 for these three examples illustrate the necessity of model size reduction for nonlinear analysis. The CPU/time steps ratio increased by 42% when comparing JEM-PM berthing to S3/S4 segment berthing, while the nonlinear analysis model size increased by 31%. Although the total number of CGAP elements increased from 9 to 16 between these events, previous studies have shown that this magnitude of increase does not significantly affect solution time. Comparison of ULC berthing and JEM-PM berthing in Table 1 shows that the CPU/time steps ratio increased by 127% while the nonlinear analysis model size only increased by 57%. The number of CGAP elements for these events was identical. These results indicate that model reduction is critical for computationally efficient solution of nonlinear impacts on large structures.

The inclusion of bisection and dynamic matrix updates in the nonlinear analysis proved effective for obtaining convergent solutions for all examples. However, adjustment of the convergence criteria was necessary in the ULC analysis because of the high gap closed stiffness employed. In the S3/S4 segment and JEM-PM analyses, the gap closed stiffness were of the same order as that of the on-orbit structure interface, therefore use of a more stringent convergence criteria was possible.

CONCLUSIONS

An accurate and computationally efficient procedure using MSC/NASTRAN has been presented for modelling and analysis of impact events for large space structures. Three different examples with widely varying structural configurations, interface designs, and analysis set sizes were presented to illustrate its use.

Reduction of the berthing module to rigid mass properties provided conservatism in the impact force magnitudes while reducing the overall analysis set size. Modelling of the berthing interface with a minimum number of CGAP elements and inclusion of berthing module interface flexibility on the gap closed stiffness, KA, allowed the use of larger time steps, improved solution convergence, and helped minimize solution CPU time. Use of CMS techniques to develop the nonlinear model provided the single most important reduction in nonlinear analysis time by reducing the analysis set by 79-82% from the structural analysis model. The inclusion of bisection and dynamic matrix updates in the nonlinear analysis proved effective for obtaining convergent solutions for all examples. Finally, use of modal transient analysis and the mode displacement data recovery method minimized loads recovery time for the large number of response items.

FURTHER STUDIES

Several variations of this procedure have been studied to date with success. The first involves flexible rather than rigid representation of the berthing module. The berthing module was reduced by use of CMS, where the contact points were held in the boundary set of the superelement. Initial velocities were then assigned to the reduced berthing module boundary points, and the nonlinear and modal transient analyses were performed as described previously. The second variation involves the use of NOLIN1 elements for modelling interface mechanisms where CGAP elements cannot be directly applied. Combinations of NOLIN1 and CGAP elements in parallel, and NOLIN1 elements alone were used to model a preloaded plunger mechanism, and this model will be used in future berthing analyses.

ACKNOWLEDGMENTS

The development of the procedure described herein was conducted under Contract NAS9-18200 for the NASA Johnson Space Center and Contract HX 3222 for Boeing Defense & Space Group. The authors wish to acknowledge the efforts of H. K. Nguyen and J. D. Qualls, formerly of MDA, who participated in the early development of this method, and S. L. Shein of MDA for suggestions and support.

REFERENCES

- [1] *Space Station Program Structural Design Loads Data Book, Volume 1: Structural Design Loads Analysis Criteria.* NASA Document Number SSP30800. August, 1993.
- [2] *MSC/NASTRAN Users Manual, Version 67,* The MacNeal-Schwendler Corporation, Los Angeles, CA, August 1991.
- [3] "MSC/NASTRAN Material and Geometric Nonlinear Analysis (Version 66) Seminar Notes," The MacNeal-Schwendler Corporation, Los Angeles, CA, September 1991.
- [4] "MSC/NASTRAN Dynamics Seminar Notes," The MacNeal-Schwendler Corporation, Los Angeles, CA, September 1991.
- [5] "MSC/NASTRAN Superelement Analysis Seminar Notes," The MacNeal-Schwendler Corporation, Los Angeles, CA, September 1991.
- [6] Craig, Roy R., Jr., *Structural Dynamics, An Introduction to Computer Methods,* John Wiley & Sons, Inc., 1981.
- [7] Kim, H. M., Bartkowicz, T. J., and VanHorn, D. A., "Data Recovery and Model Reduction Methods for Large Structures," Proceedings of 1993 MSC World Users' Conference, The MacNeal Schwendler Corporation, Los Angeles, CA, 1993.

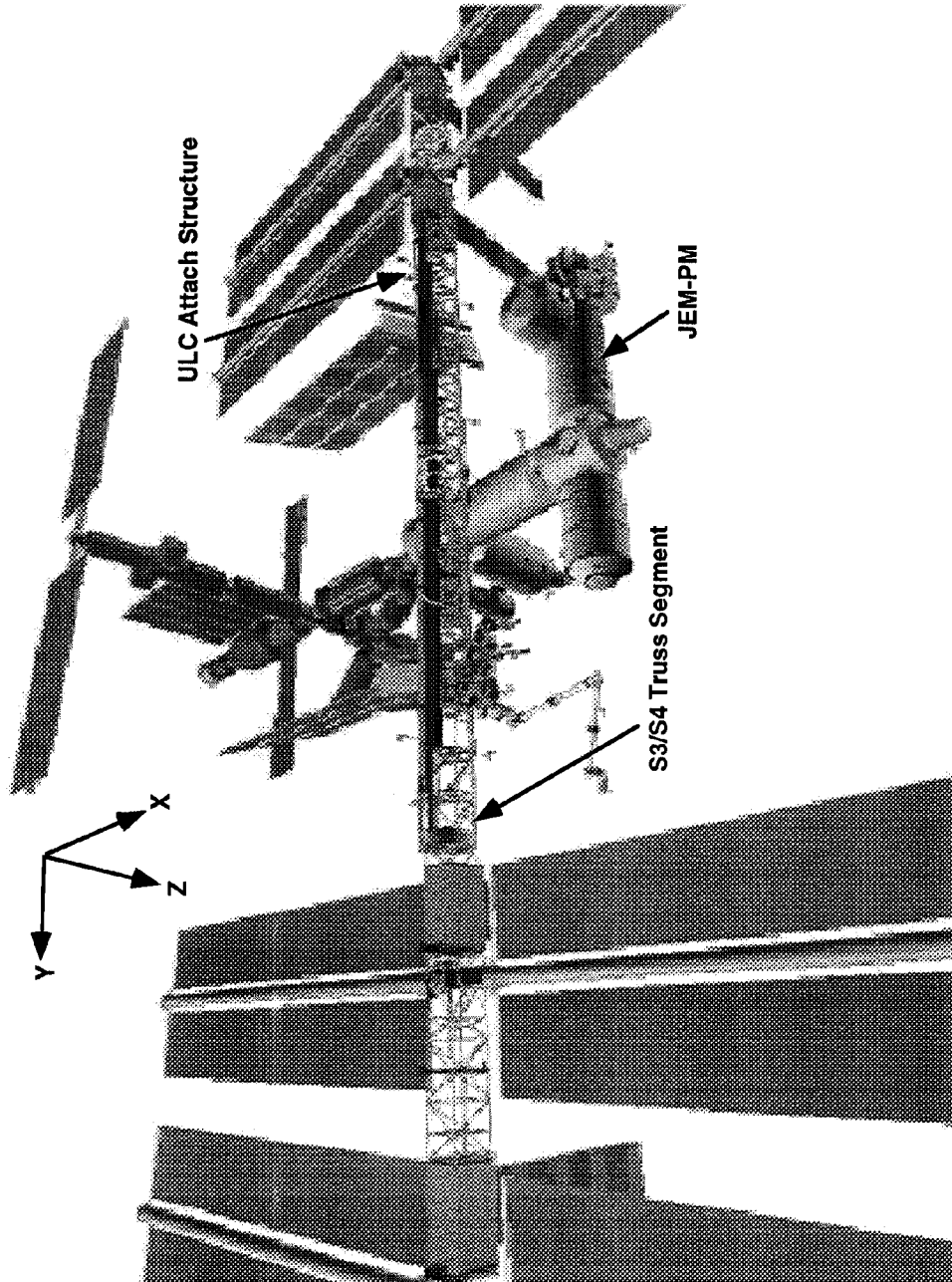


Figure 1: International Space Station Alpha (Assembly Complete)

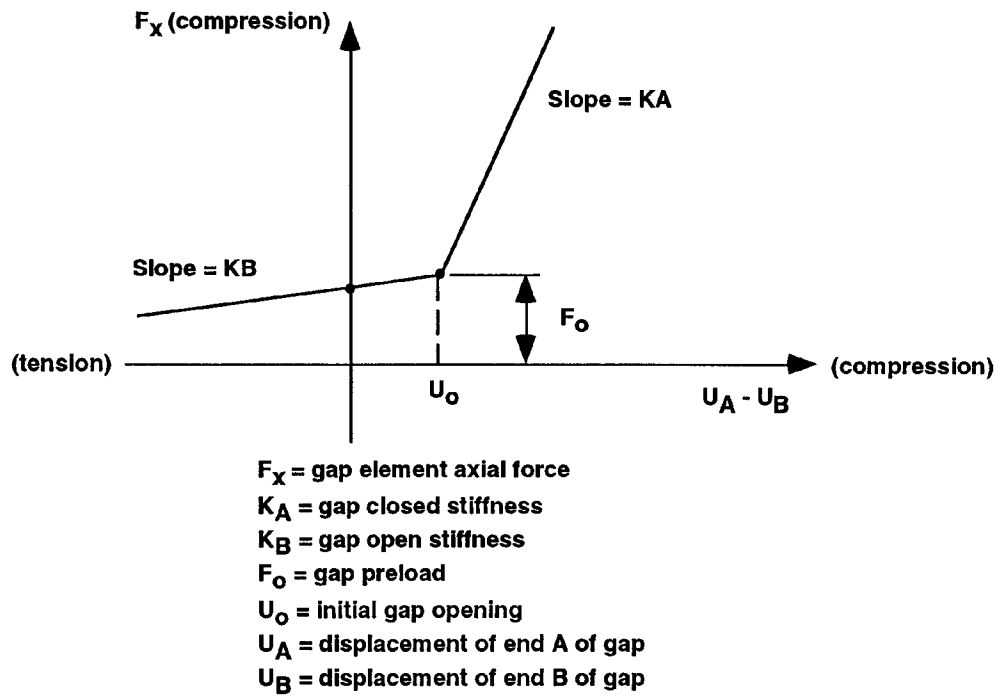


Figure 2: CGAP Element Force-Deflection Curve for Nonlinear Analysis

Table 1: Model and Analysis Parameters

| Model/Analysis Parameters | S3/S4 Segment Berthing | JEM-PM Berthing | ULC Berthing |
|--|-------------------------------|------------------------|---------------------|
| On-orbit Configuration Approx. Weight (lbs) | 645,000 | 694,000 | 1,025,000 |
| Berthing Module Approx. Weight (lbs) | 31,000 | 39,000 | 19,000 |
| Structural Analysis Model DOF | 3,918 | 5,727 | 9,307 |
| Nonlinear Analysis Model DOF | 832 | 1,091 | 1,716 |
| Total CGAP Elements | 9 | 16 | 16 |
| Nonlinear Analysis Integration Time Step (seconds) | 0.01 | 0.0025 | 0.01 |
| Nonlinear Analysis Number of Time Steps | 500 | 1600 | 500 |
| Nonlinear Analysis CPU Time (CPU seconds*) | 423 | 1,920 | 1,363 |
| Nonlinear Analysis CPU/Time Steps Ratio | 0.85 | 1.20 | 2.73 |
| Structural Analysis Simulation Time (seconds) | 82.0 | 82.0 | 82.0 |
| Total Structural Analysis Recovery Items | 6,400 | 10,500 | 14,500 |

*CPU seconds on a Cray Y-MP Supercomputer

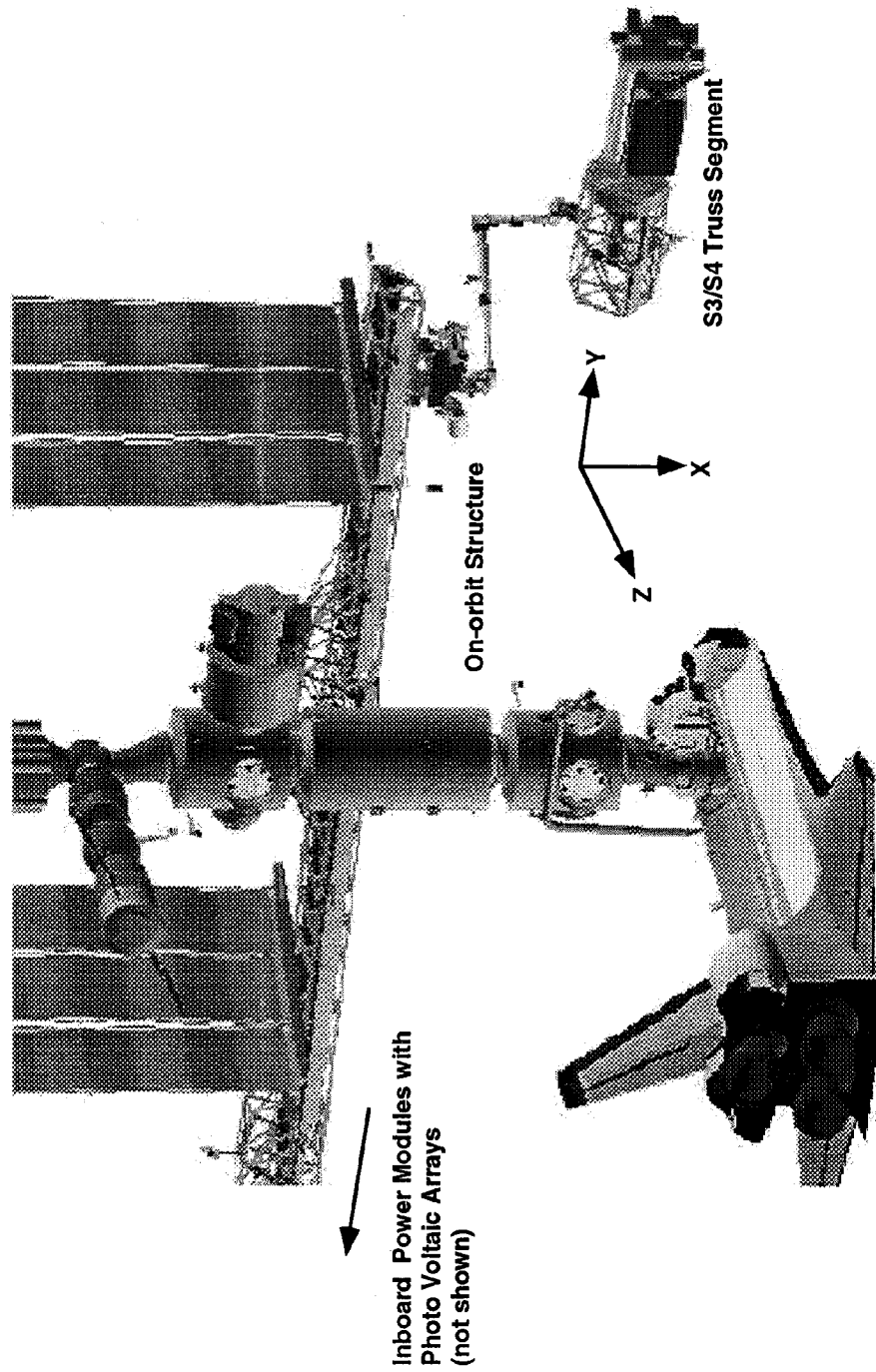


Figure 3: S3/S4 Truss Segment Berthing

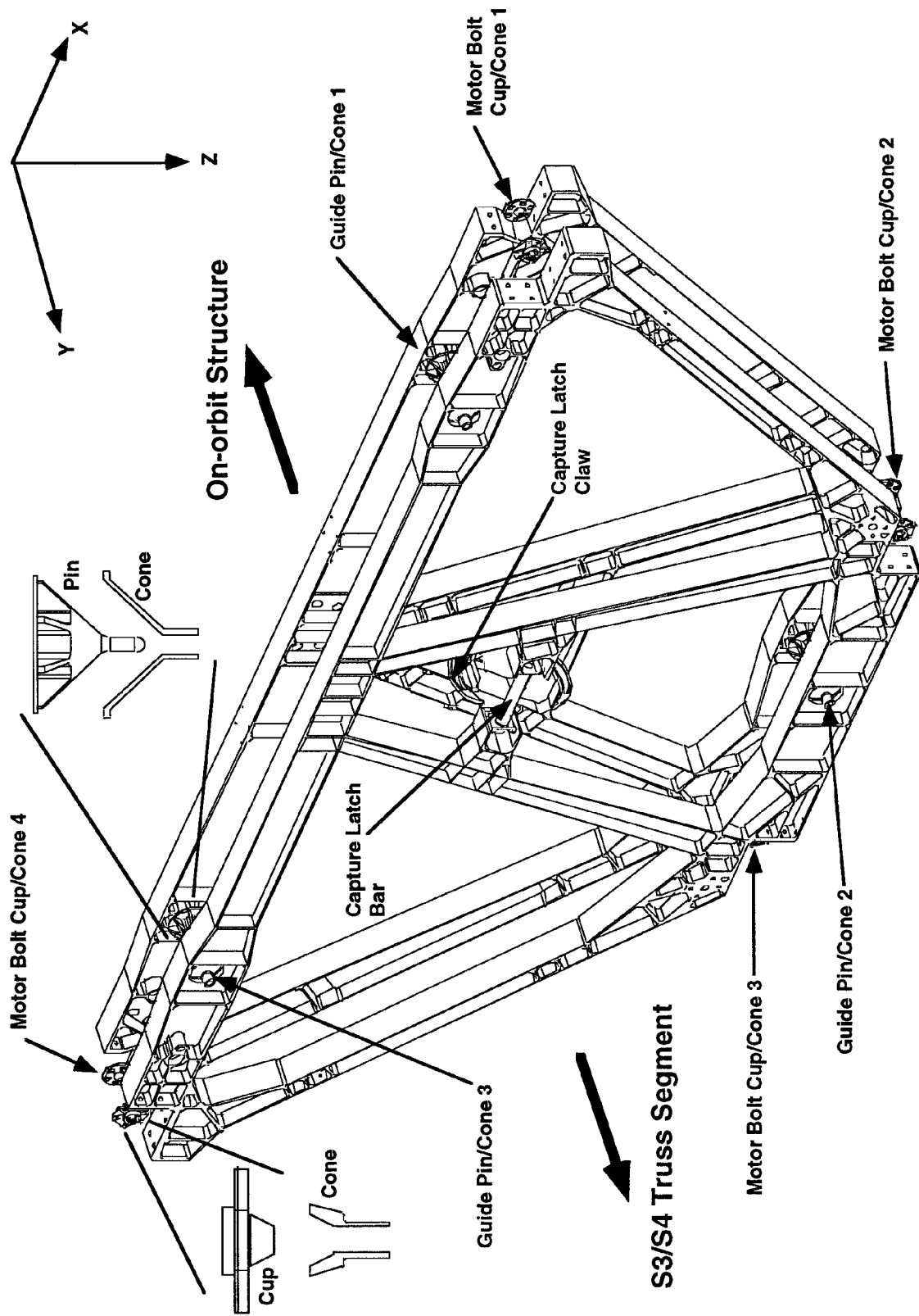
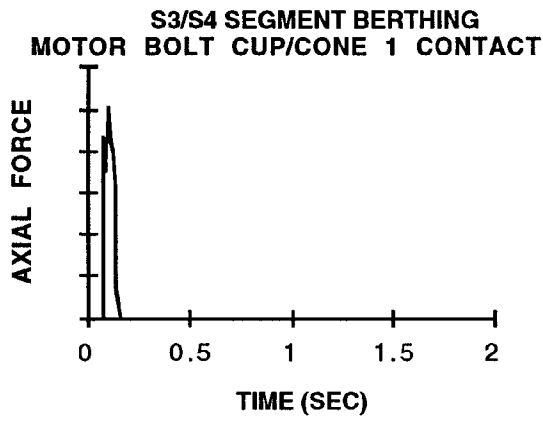
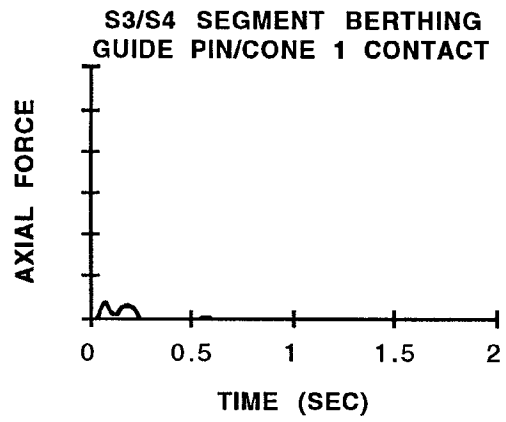


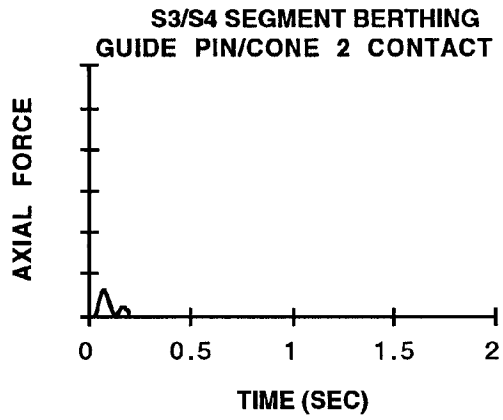
Figure 4: Segment-to-Segment Attach System



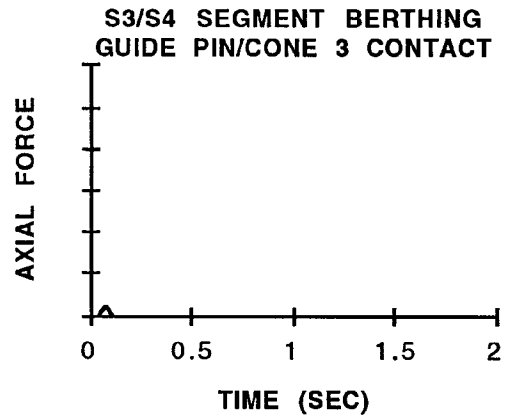
(a)



(b)



(c)



(d)

Figure 5: S3/S4 Truss Segment Berthing Impact Forces

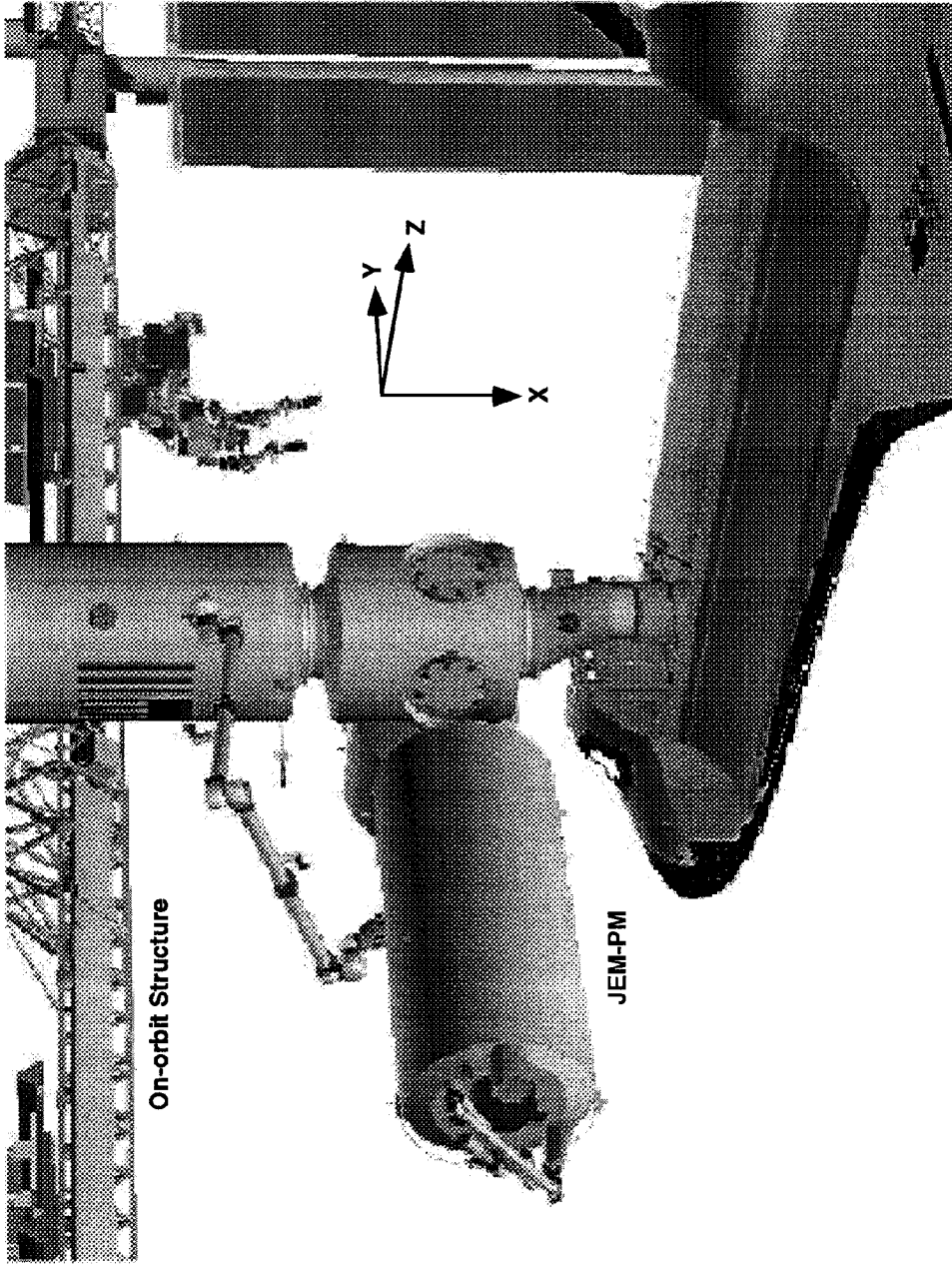


Figure 6: Japanese Experiment Module - Pressurized Module Berthing

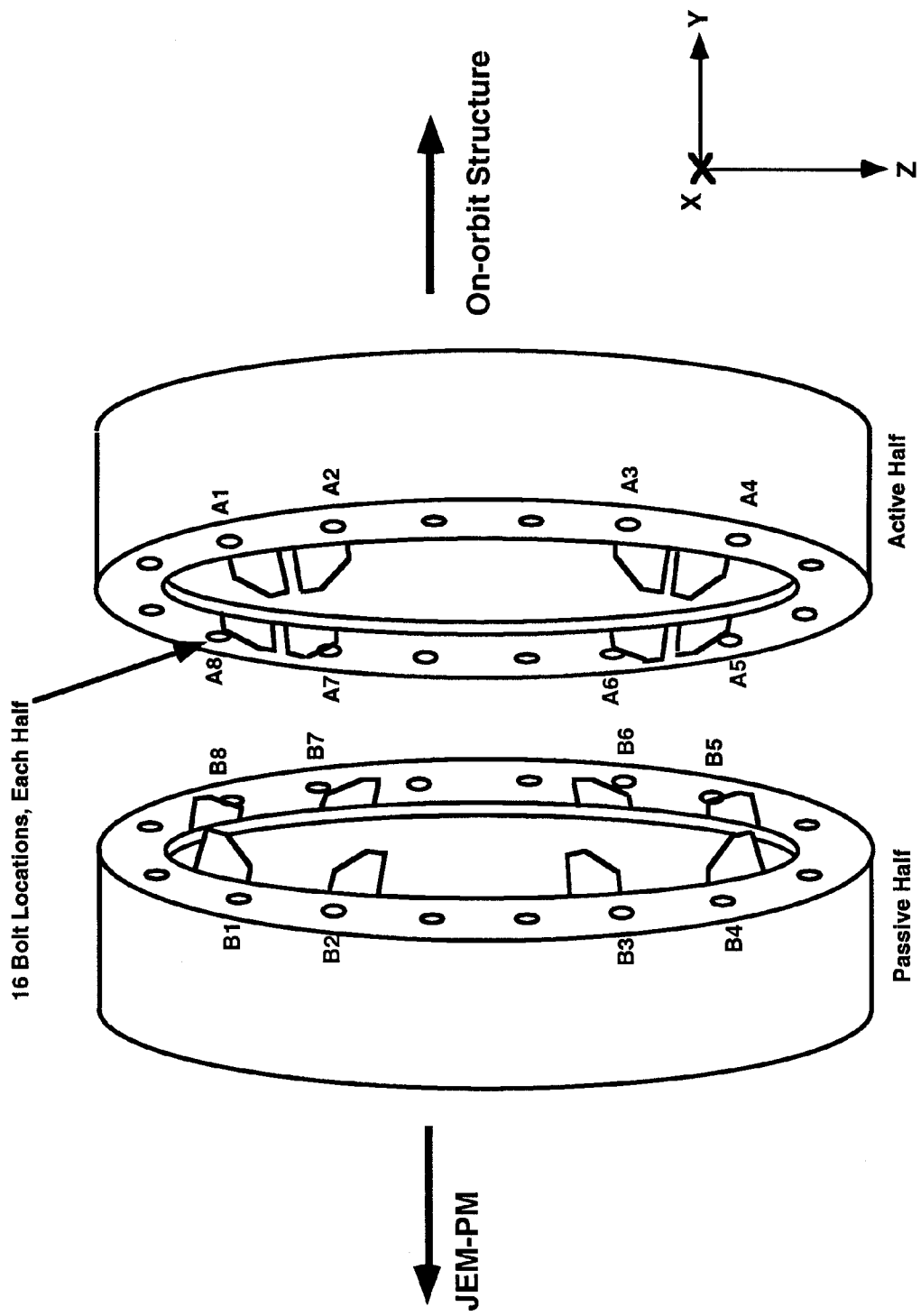


Figure 7: Common Berthing Mechanism

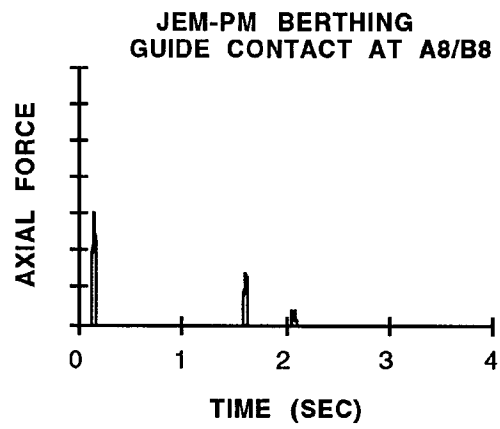
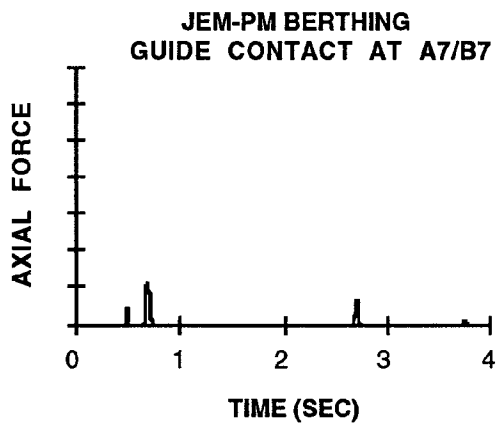
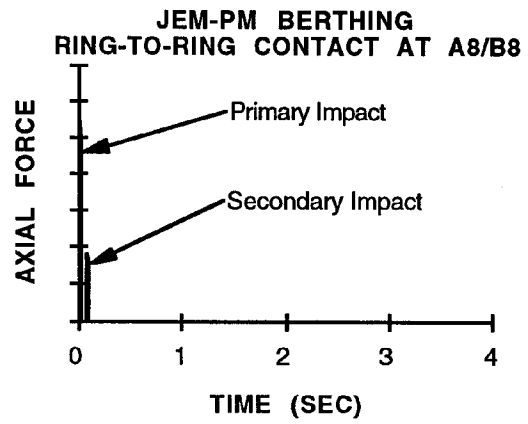
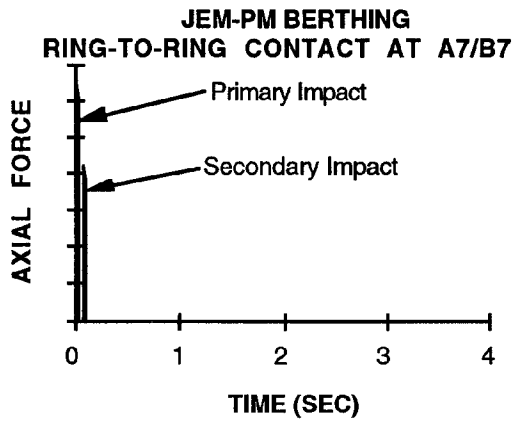


Figure 8: JEM-PM Berthing Impact Forces

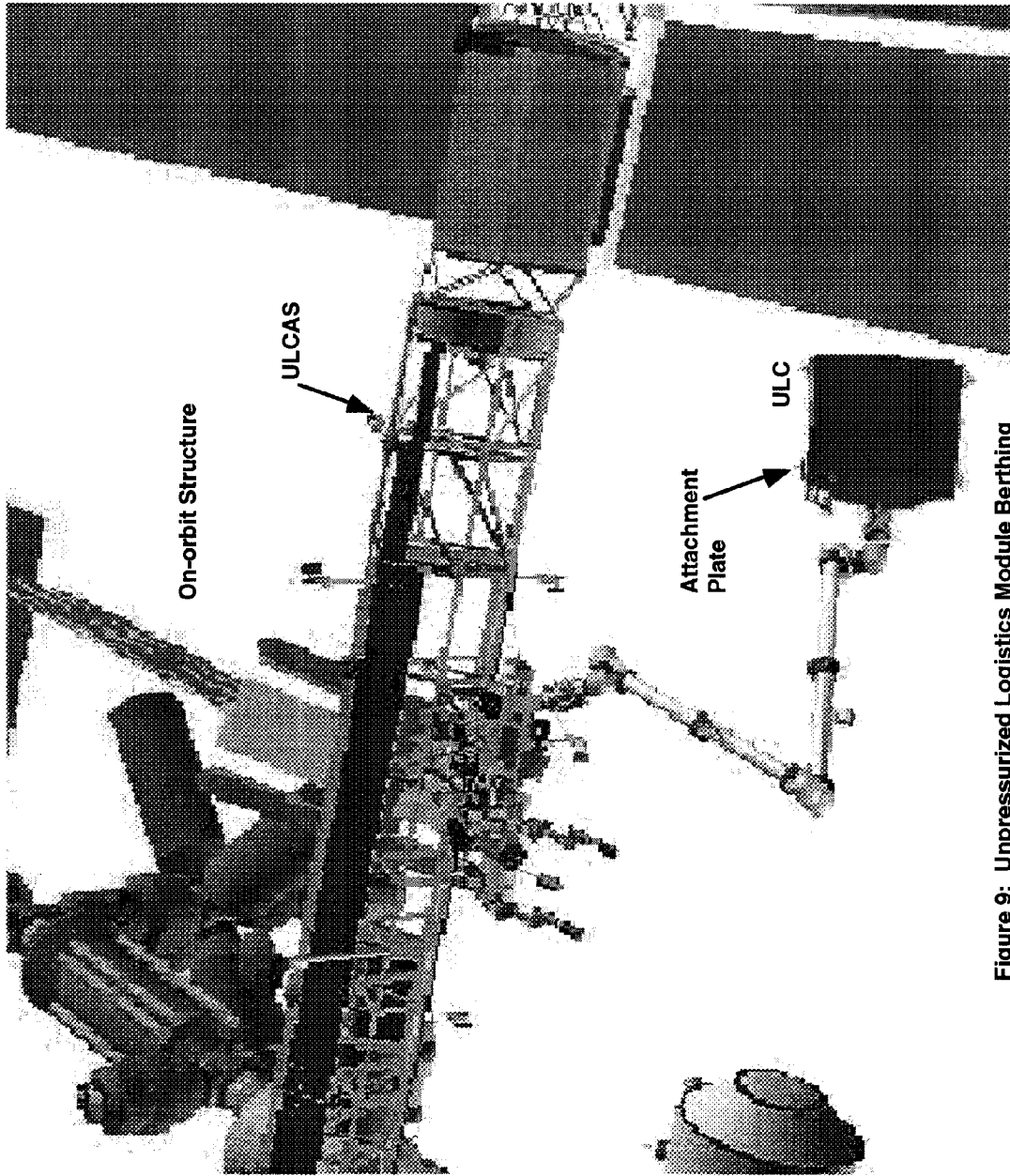


Figure 9: Unpressurized Logistics Module Berthing

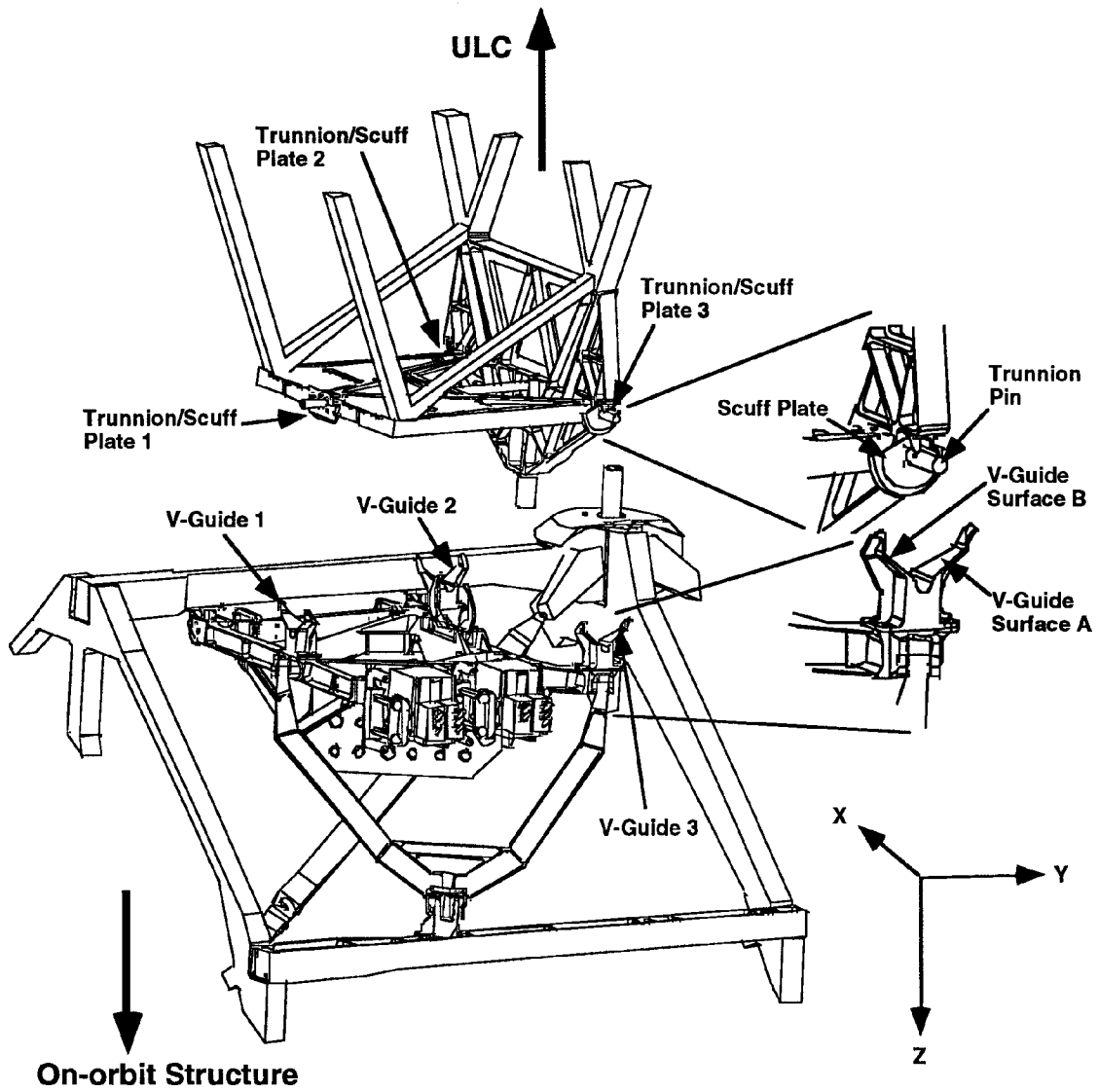


Figure 10: Unpressurized Logistics Carrier Attach Structure

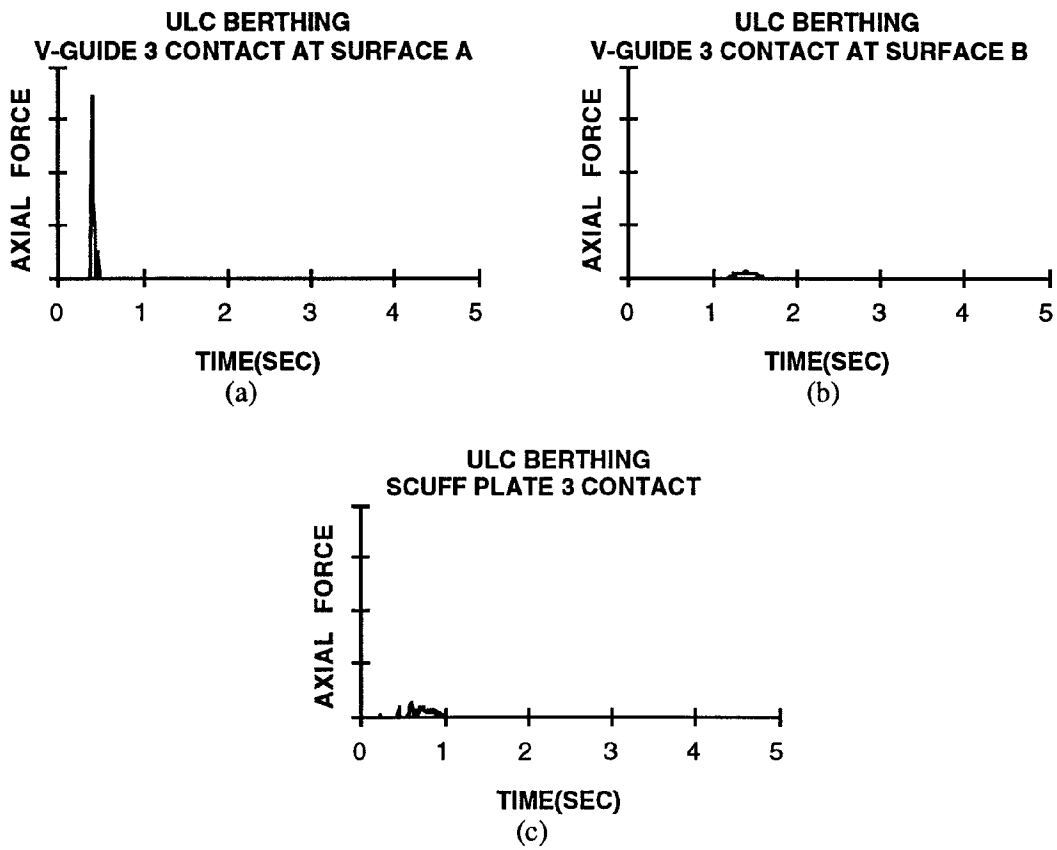


Figure 11: ULC Berthing Impact Forces